

● *Original Contribution*

TISSUE DISPLACEMENTS DURING ACUPUNCTURE USING ULTRASOUND ELASTOGRAPHY TECHNIQUES

HELENE M. LANGEVIN,* ELISA E. KONOFAGOU,^{||} GARY J. BADGER,[†] DAVID L. CHURCHILL,*
JAMES R. FOX,[‡] JONATHAN OPHIR[¶] and BRIAN S. GARRA[§]

Departments of *Neurology, [†]Medical Biostatistics, [‡]Orthopaedics & Rehabilitation and [§]Radiology, University of Vermont, Burlington, VT, USA; ^{||}Department of Biomedical Engineering, Columbia University, New York, NY, USA; and [¶]Department of Radiology, University of Texas Medical School at Houston, Houston, TX, USA

(Received 9 February 2004; revised 30 June 2004; accepted 8 July 2004)

Abstract—Acupuncture needle manipulation has been previously shown to result in measurable changes in connective tissue architecture in animal experiments. In this study, we used a novel *in vivo* ultrasound (US)-based technique to quantify tissue displacement during acupuncture manipulation in humans. B-scan ultrasonic imaging was performed on the thighs of 12 human subjects at different stages of needle motion, including varying amounts of rotation, downward and upward movement performed with a computer-controlled acupuncture needling instrument. Tissue displacements, estimated using cross-correlation techniques, provided successful mapping and quantitative analysis of spatial and temporal tissue behavior during acupuncture needle manipulation. Increasing amounts of rotation had a significant linear effect on tissue displacement during downward and upward needle motion, as well as on rebound tissue displacement after downward needle movement. In addition to being a valuable tool for studies of acupuncture's mechanism of action, this technique may have applications to other types of needling including biopsies. (E-mail: Helene.langevin@uvm.edu) © 2004 World Federation for Ultrasound in Medicine & Biology.

Key Words: Ultrasound, Elastography, Tissue displacement, Acupuncture, Acupuncture needle manipulation, Connective tissue.

INTRODUCTION

Despite its increasing worldwide use, acupuncture's therapeutic mechanism remains poorly understood (NIH 1997). An important and frequently overlooked aspect of acupuncture treatments is the manual needle manipulation performed by acupuncturists after needle insertion. Manipulation consists of varying amounts of rapid up-and-down (referred to as "lifting and thrusting") and rotational needle movements. The amount and duration of these movements depend on the clinical presentation, the training of the acupuncturist and the point needled (Cheng, 1997; Helms, 1995; O'Connor and Bensky 1991). Acupuncturists believe that the type, speed, amplitude, duration and periodicity of needle movements all influence treatment outcome. Currently, however, there is no scientific explanation linking specific needle manipulation techniques to therapeutic effects. In particular, the rationale for the very common and

ancient practice of using a combination of rotation, lifting and thrusting remains unknown.

Recently, we have proposed a new model for the therapeutic effect of acupuncture involving connective tissue mechanotransduction (Langevin et al. 2001a). This model is supported by human and animal experiments showing that, during needle rotation, connective tissue winds and tightens around the needle, thus increasing the force necessary to pull the needle out of the skin (Langevin et al. 2001b, 2002). Further, we showed that the network formed by interstitial or "loose" connective tissue may correspond to the acupuncture meridian network (Langevin and Yandow 2002). A new and challenging way to think about acupuncture therefore has emerged: biochemical effects deriving from mechanical stimulation of connective tissue and potential spreading of these effects along connective tissue planes may explain acupuncture's therapeutic effect as well as traditional acupuncture theory.

Our previous studies in humans relied on measuring needle force and torque during needle movement. Al-

Address correspondence to: Helene M. Langevin, M.D., Department of Neurology, Given C 423, 89 Beaumont ave, Burlington VT 05405 USA. E-mail: Helene.langevin@uvm.edu

though needle forces can give important information on the strength of the bond between tissue and needle and how this bond is affected by needle manipulation, they do not give information on tissue behavior away from the needle. This is important for a number of reasons: first, measuring the spatial extent of tissue movement induced by needle manipulation will allow investigation of whether acupuncture effects are more pronounced along the path of acupuncture meridians and/or connective tissue planes; and second, this *in vivo* work will permit translation of *in vitro* mechanotransduction research, thus giving insights into the tissue biochemical events occurring in response to needle manipulation.

Ultrasound constitutes an ideal medium for evaluating the biomechanical effects of needle manipulation on tissue. Ultrasound has the unique advantage of yielding both images of tissue morphology and biomechanical information. First, in humans, inserting the acupuncture needle under sonographic B-scan visualization allows identification of anatomical details (*i.e.*, tissue layers; skin, subcutaneous tissue, perimuscular fascia, muscle) penetrated by the needle (Langevin and Yandow 2002). Second, continuous US recording during acupuncture needle movement (insertion, manipulation and pullout) permits quantitative tissue motion analysis at a varying distance away from the needle using off-line elastography techniques. Elastography aims at quantifying a mechanical response or the mechanical property of tissues resulting from a mechanical stimulus, generated internally or externally (Ophir et al. 1991, Ophir et al. 1999). In traditional elastography and other elasticity imaging techniques, an external force or displacement is applied, such as a quasistatic compression (Ophir et al. 1991) or vibration (Levinson et al. 1995). As a result, the whole target is under motion simultaneously. Differential techniques, such as strain or velocity, therefore need to be employed to differentiate between tissues based on their distinct mechanical properties (Ophir et al. 1999). Another way of probing tissues for spatial elasticity mapping is to use an internally applied mechanical stimulus inducing a localized tissue response (*i.e.*, concentrated in a specific region inside the tissue). Localized displacement, static or dynamic, has been shown to be directly related to the underlying modulus when the force is exerted over a small area (Krouskop et al. 1998). In the area of mechanical testing, a very small piston is customarily used so that the semi-infinite assumption for the medium is satisfied and the models used for estimation of the mechanical property are verified (Krouskop et al. 1998). In the area of US, a new focus of elasticity imaging has been to use the ultrasonic radiation force generated through the change in momentum of the ultrasonic wave during propagation within the tissue. This force can then be concentrated over the focal area of the

transducer, that is usually of the order of a few square millimeters. As a result, borrowing again from mechanical testing principles, the images that are generated depict only the displacement amplitude as a result of the generation of the radiation force (Barannik et al. 2002; Konofagou and Hynynen 2003; Nightingale et al. 2001; Walker et al. 2000). In this study, we have developed a new technique combining computer-controlled acupuncture needling with ultrasonic signal-processing methods to quantify tissue displacement during acupuncture needle manipulation *in vivo*. Unlike traditional elastography that typically uses an externally applied compression and derives tissue strain and stiffness estimation, we used a controlled needling stimulus to produce tissue movement. In elastography using external compression, the whole tissue being insonified is perturbed and therefore a differential parameter (*e.g.*, strain) needs to be used to detect the tissues undergoing higher (or lower) motion. In this study, comparing the effect of different needle motion conditions, the highly localized nature of the mechanical stimulus produced by the needle allowed us to use displacement instead of other parameters such as strain to quantify tissue motion. An advantage of using tissue displacement in this case is that it is significantly less noise-prone than tissue strain estimation due to the elimination of the noise-amplifying gradient operation.

Our previous work shows that, during needle rotation, connective tissue winds and tightens around the needle (Langevin et al. 2002). In this paper, we propose that rotation acts by increasing the mechanical coupling between needle and tissue, thereby preventing the needle from sliding through the tissue during subsequent needle manipulation. This tighter mechanical coupling would cause increased pulling of tissue during lifting and thrusting of the needle, thus making mechanical tissue stimulation more effective.

The aims of this study, therefore, were the following. First, use US elastography techniques to show that different types of acupuncture needle manipulation cause characteristic patterns of tissue displacement that can be mapped spatially and temporally. Second, test the hypothesis that increasing amounts of rotation result in increasing tissue displacement during upward and downward needle movement. Testing this hypothesis will provide quantitative data that can be used to understand the rationale for performing appropriate acupuncture techniques, which may improve treatment effectiveness as well as increase our understanding of the mechanisms underlying this ancient form of therapy. Finally, we aim to demonstrate the general feasibility of using the movement of a needle as an effective mechanical stimulus for analysis of tissue displacement. This technique may be used with different types of needles, including those used to obtain biopsies, and future studies may potentially

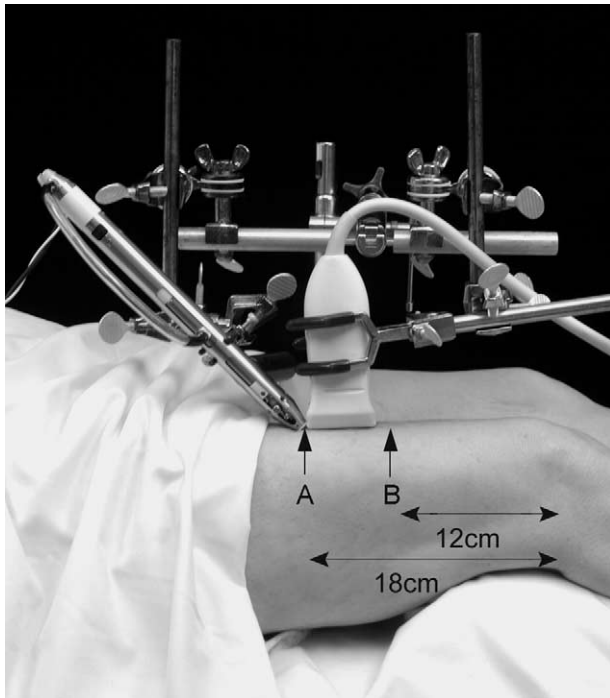


Fig. 1. Experimental setup with acupuncture needling instrument (left) and US transducer (right). Also indicated are needling locations A and B on the anterior thigh, respectively, located 18 cm and 12 cm rostral to the patella.

reveal important differences between normal and diseased tissues that may be useful diagnostically.

METHODS

Equipment

In vivo ultrasonic imaging was performed on the thighs of 12 healthy human subjects at different stages of needle motion performed by a computer-controlled acupuncture needling instrument (Fig. 1). The needling instrument was custom-made as previously described (Langevin *et al.* 2001b). Disposable stainless-steel needles (Seirin, Japan, 0.25 mm in diameter and 40 mm in length) were used. The US equipment consisted of a System Five (GE-Vingmed, Norway) scanner equipped with a linear-array transducer. Ultrasound frequency was 6.9 MHz. The needling instrument and US transducer were placed in a clamp system such that the transducer was perpendicular to the skin and the needling instrument was at a 45° angle to the transducer (Figs. 1 and 3).

Study design, randomized variables and needling parameters

Each subject underwent four separate needling procedures, one at each of four points on the thigh: two

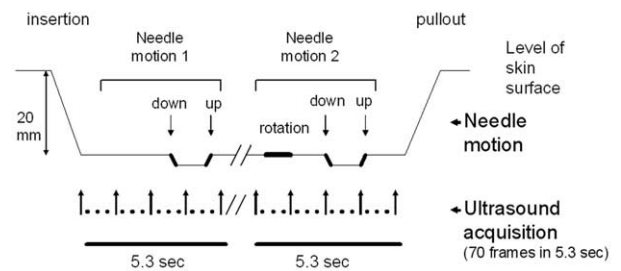


Fig. 2. Timing of needle motion and US acquisition (see text).

distal and two proximal points bilaterally, respectively located 18 cm (location A) and 12 cm (location B) proximal to the middle of the superior edge of the patella. Each needling procedure consisted of the following sequence (Fig. 2): needle insertion to a depth of 28 mm; a 3 s dwell time followed by downward and upward 2 mm longitudinal needle motion (needle motion 1); varying amounts of needle rotation (0, 4, 8 and 16 unidirectional clockwise revolutions) followed by downward and upward 2-mm longitudinal needle motion (needle motion 2); needle pullout. Needle rotation and longitudinal motion speeds were 16 revolutions /s and 10 mm/s, respectively. Needle dwell times between downward and upward needle motions and from rotation to beginning of downward needle motion all were 1 s. Because the needling instrument and US probe were at a 45° angle to each other, the length of the vector corresponding to the projection of the 2 mm upward and downward needle motions onto the axis of the ultrasound beam was $2 * \cos(45) = 1.41$ mm (Fig. 3b). The number of needle revolutions was randomized in a Latin square design, such that, within each subject, each of the four points received a different rotation condition (see Statistical methods section below).

Data acquisition

During longitudinal needle movements, a 500 g capacity load cell built into the acupuncture needling instrument recorded the force required to linearly advance and retract the needle (thereafter referred to as “needle force”). During needle rotation, an estimate of rotational torque (thereafter referred to as “needle torque”) was obtained by measuring the amount of current delivered to the servomotor generating rotation.

The GE Vingmed system allows for the acquisition of the raw ultrasonic data, or radiofrequency (RF) data. To estimate the displacement that occurred between successive frames, the RF data are used because it has been shown that RF data provide a far better precision in the displacement estimation than B-scan data (Hein and O’Brien 1993). The RF data are stored and used following digitization by the Vingmed system at a sampling frequency of 20 MHz.

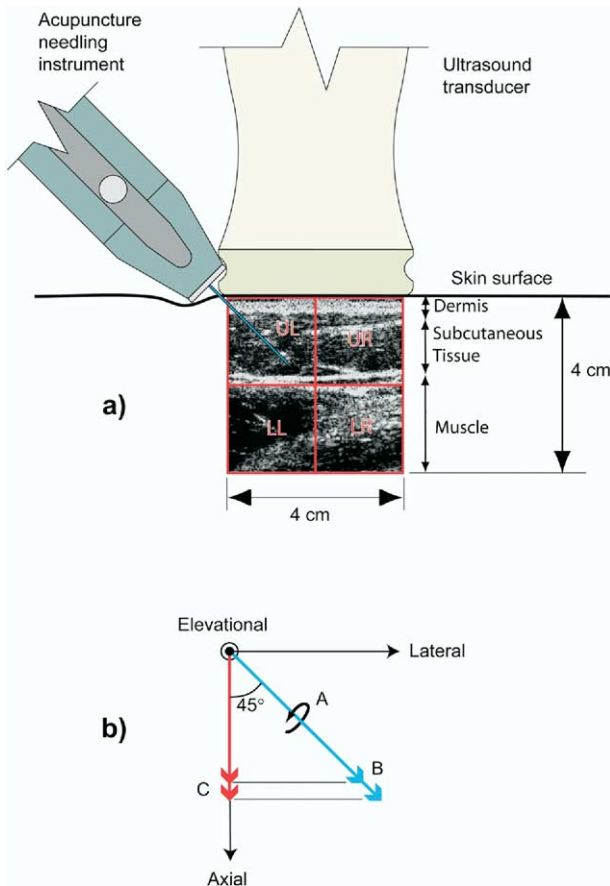


Fig. 3. (a) Positioning of US transducer and needle. The US image is divided into four quadrants: Upper left (UL) including needle, lower left (LL), upper right (UR) and lower right (LR). (b) Vector diagram of needle motion relative to the plane of the US image. A = needle insertion distance (28 mm); B = 2 mm downward needle motion; C = 1.41 mm projection of downward needle motion vector onto the axis of propagation of the US beam. Curved arrow represents needle rotation.

Two separate cine-loops, each consisting of 70 RF scans, were acquired continuously during each needling procedure at the rate of 13.2 frames/s. The first and second cine-loops included needle motion 1 and needle motion 2, respectively. Mean (\pm SD) dwell time between the end of the first and the beginning of the second cine-loop was 309 ± 43 s. This dwell time was necessary to transfer the first RF data file from the US scanner to the PC buffer. During this dwell time, the needle was left undisturbed in the tissue.

Data processing

Tissue displacements were estimated using successive ultrasonic RF data and cross-correlation techniques previously described by Ophir et al. (1991) with a 2-mm window and a window overlap of 60%. Therefore, in this paper (except where stated otherwise), the term “dis-

placement” refers to the incremental axial (i.e., along the propagation of the US beam or top to bottom on all images shown) motion that the tissue undergoes between two successively acquired US frames (i.e., after 76 ms have elapsed). Cine-loop displacement images were generated off-line during and between the different needle movements. For the purpose of analysis, the US image was divided into four quadrants, upper left (UL), lower left (LL), upper right (UR) and lower right (LR) (Fig. 3). The needle was inserted in the upper left quadrant of the US frame so that 1. the spatial extent of the effect of the needling could be assessed and 2. the motion of the tissue away from the needle could be compared with that of tissue adjacent to the needle.

Raw data for needle force, needle torque and tissue displacement, as well as needle motion, are graphically represented in Fig. 4. The following outcome measures were used for statistical analysis. For tissue displacement, in each image, we calculated an average displacement within each US image quadrant. We then identified the peak tissue displacement value over the range of frames of interest (i.e., during rotation, upward and downward needle motion). For needle torque, we used peak torque during rotation. For needle force, we calculated the difference between the force at the beginning and end of each upward or downward needle motion.

Finally, to calculate the total tissue displacement through one full rotation, upward and downward motion, cumulative displacement was calculated from the beginning to the end of each needle motion.

Statistical methods

Repeated measures analyses of variance (ANOVA) were used to test for differences in mean torque, force and displacement across rotation conditions (0, 4, 8, 16), needling locations (proximal vs. distal) and sides (right vs. left). The analyses reflected the randomization protocol, which corresponded to a replicated Latin-square design. The 12 subjects constituted three replicates of a 4^3 design. That is, the four rotation conditions were balanced across the four needling areas (two locations \times two sides) for each set of four subjects. Because the rotation condition represented a quantitative factor, orthogonal polynomials were used to partition its overall effect (sums of squares) into components representing linear, quadratic and cubic trends (Montgomery 1991). The contrast representing the linear component was used to test specifically for increasing or decreasing effects as a function of number of needle rotations. Tests for quadratic and cubic trends are not presented, as there was no evidence of nonlinearity for any of the outcome measures examined. Each outcome measure was examined separately for needle motion 1 (prerotation), needle motion 2 (postrotation) and their difference. T-tests using

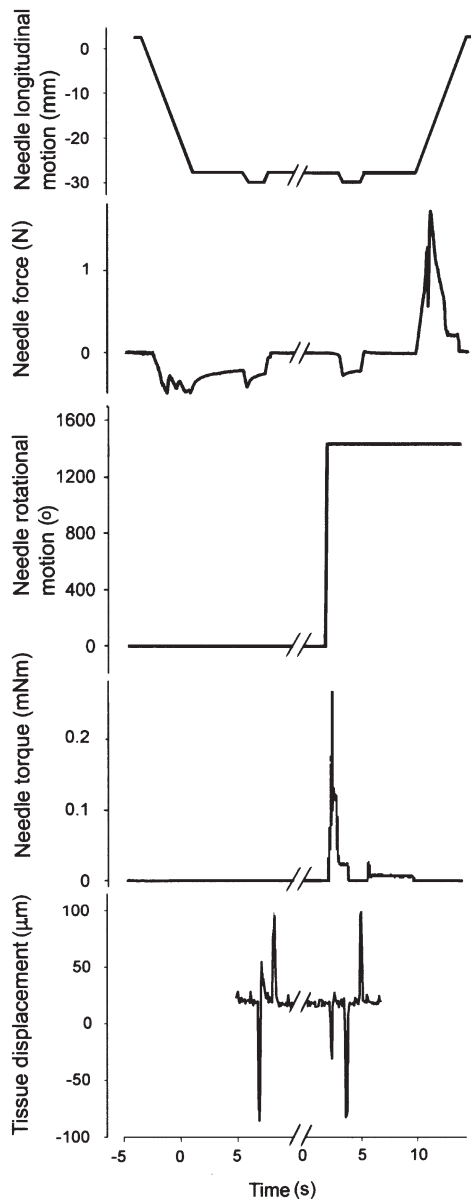


Fig. 4. Graphic representation of needle longitudinal motion, needle force, needle rotational motion, needle torque and tissue displacement measurements.

the residual mean squares from the ANOVA were used to determine if mean torque, force and displacement were significantly different from zero and to test for differences between needle motion 1 and needle motion 2 within each rotation condition.

RESULTS

Needle motion 1

During needle motion 1 (before needle rotation), there was no evidence of any differences across points randomized to subsequently receive different rotation

conditions during needle motion 2 (Table 1). There was evidence that downward and upward needle motion, respectively, caused significant downward and upward tissue displacement in all four quadrants of the US image ($p < 0.001$ for all outcome measures).

Needle motion 2

During needle rotation, tissue displacement increased in amplitude by up to five-fold, and in spatial extent by up to four-fold, compared with baseline. Figure 5 shows sequential displacement images with and without rotation. The extent of tissue displacement during needle rotation is evident in Fig. 5b, frames 4 to 6. Figure 6 illustrates the gradual increase in tissue displacement occurring during increasing amounts of rotation (Fig. 6 left column).

Increasing the amount of rotation resulted in increasing needle torque ($p < 0.001$) (Table 2), as well as increasing mean tissue displacement during rotation (Fig. 7). This result was significant for each individual image quadrant (Table 2), and when averaged over the whole US image ($p < 0.001$).

After needle rotation, increasing amount of rotation increased needle force ($p < 0.001$) (Fig. 8) and overall mean tissue displacement during downward ($p < 0.01$) and upward ($p < 0.01$) needle motion (Fig. 9). Increasing amount of rotation caused significantly increased tissue displacement within all individual image quadrants except for downward displacement in the lower right quadrant (Table 2).

Rebound tissue displacement after downward needle motion

Needle rotation resulted in decreased tissue rebound following the downward portion of motion 2 (Fig. 10). Increasing the amount of rotation significantly decreased overall mean rebound tissue displacement ($p < 0.05$) (Fig. 11). In individual US image quadrants, there was a significant effect of rotation in the upper left quadrant (including needle) and lower left (below needle), but not in the upper right and lower right (lateral to needle) (Table 2).

Differences between needle motions 1 and 2

For upward needle motion, there were significant differences in tissue displacement between needle motions 1 and 2 with no rotation (Fig. 9). Thus, tissue displacement during upward needle movement was lower during motion 2 than during motion 1 when no rotation occurred. A marked difference between motions 1 and 2 with no rotation also was seen with rebound tissue displacement (Fig. 11).

There were no significant effects of needling location (A vs. B) or side of the body (right vs. left) on any of the measurements.

Table 1. Needle force and tissue displacement during needle motion 1 (prior to needle rotation) across points randomized to the four rotation conditions

		Randomized rotation conditions				Mean*	p value [†]	
		0	4	8	16			
Downward needle motion	Force (N)	-0.37 ± 0.04	-0.34 ± 0.03	-0.37 ± 0.03	-0.35 ± 0.03	-0.36 ± 0.01	0.82	
	Disp (μm)	UL	-77.3 ± 6.8	-79.5 ± 5.7	-78.2 ± 6.2	-75.4 ± 5.7	-77.6 ± 2.5	0.95
		LL	-81.7 ± 8.9	-99.0 ± 9.2	-89.9 ± 10.8	-92.4 ± 8.9	-90.8 ± 4.1	0.54
		UR	-16.8 ± 3.6	-16.1 ± 2.9	-17.9 ± 3.0	-20.4 ± 3.4	-17.8 ± 1.4	0.72
		LR	-39.4 ± 5.6	-35.8 ± 3.7	-37.0 ± 4.2	-38.2 ± 5.1	-37.6 ± 2.2	0.95
Overall	-53.8 ± 5.0	-57.6 ± 4.4	-55.8 ± 5.0	-56.6 ± 4.7	-55.9 ± 2.1	0.95		
Rebound	Disp (μm)	UL	24.8 ± 4.1	27.8 ± 4.8	27.7 ± 4.4	22.1 ± 3.1	25.6 ± 1.7	0.59
		LL	28.7 ± 4.9	35.1 ± 6.9	28.0 ± 4.6	26.0 ± 2.9	29.5 ± 2.4	0.58
		UR	2.6 ± 0.5	2.7 ± 1.1	4.0 ± 1.2	3.7 ± 1.0	3.2 ± 0.5	0.65
		LR	10.8 ± 1.7	11.7 ± 2.2	8.8 ± 2.5	8.3 ± 2.1	9.9 ± 0.9	0.55
		Overall	16.7 ± 2.0	19.4 ± 2.7	17.1 ± 2.3	15.0 ± 1.5	17.1 ± 1.0	0.50
Upward needle motion	Force (N)	0.35 ± 0.01	0.29 ± 0.02	0.37 ± 0.02	0.31 ± 0.07	0.34 ± 0.01	0.43	
	Disp (μm)	UL	68.7 ± 8.6	73.1 ± 8.6	69.7 ± 6.4	66.3 ± 6.6	69.5 ± 3.3	0.91
		LL	72.8 ± 10.4	85.3 ± 9.3	75.1 ± 8.3	74.1 ± 8.6	76.8 ± 3.9	0.66
		UR	9.5 ± 2.2	13.0 ± 2.7	10.6 ± 2.2	10.9 ± 1.9	11.0 ± 0.9	0.59
		LR	23.5 ± 4.2	27.9 ± 2.5	19.1 ± 3.8	25.1 ± 4.0	23.9 ± 1.4	0.19
Overall	43.6 ± 5.1	49.8 ± 4.7	43.7 ± 3.8	44.1 ± 4.2	45.3 ± 2.0	0.63		

Values represent mean ± SE for $n = 12$ subjects.

Tissue displacement (Disp) measurements are shown for upper left (UL), lower left (LL), upper right (UR) and lower right (LR) US image quadrants, and for the four quadrants combined (overall); units of measurement are N (force), mNm (torque) and μ (disp).

* All means are significantly different from zero ($p < 0.001$).

† Significance associated with differences across rotation conditions based on repeated measures analysis of variance F-test.

DISCUSSION

We report the first *in vivo* quantitative analysis of tissue displacement during acupuncture in humans performed by combining computer-controlled acupuncture needling and US elastography techniques. This approach allowed 1. spatial mapping and quantitative analysis of the extent of the tissue affected by acupuncture needle movement and 2. temporal monitoring of the tissue behavior as a result of the type of needle movement. We found a significant linear effect of needle rotation on tissue displacement during downward and upward needle motion, as well as on tissue rebound following downward needle motion. Needle rotation, therefore, preconditioned the tissue and modified the tissue's biomechanical behavior during subsequent longitudinal needle movement. These results are consistent with our proposed model: rotation strengthens the mechanical bond between needle and tissue, resulting in less slippage along the shaft of the needle during upward and downward needle movement. Consequently, the tissue receives greater mechanical stimulation by being pulled further up or down during each needle motion, providing a mechanistic explanation for the ancient practice of combining rotation, lifting and thrusting of the needle during acupuncture treatments.

The results of this study also demonstrate that measurable tissue displacement occurred up to 4 cm away from the needle during acupuncture in humans. Our

previous research suggests that mechanical stimulation of connective tissue during therapeutic acupuncture needling may be accompanied by long-lasting cellular and molecular events, including gene expression and extracellular matrix modification. This biomechanical "signal" may be transduced at the cellular level into biochemical effects that may be key to acupuncture's therapeutic effect. Characterizing the spatial and temporal extents of biomechanical tissue responses to needling, therefore, is an important step toward understanding the mechanism of action of acupuncture. We detected tissue displacement in all quadrants of our displacement image during all types of needle motion. This suggests that the spatial extent of the tissue affected by acupuncture needle manipulation may be substantially greater than that which we were able to measure in this study. In future work, increasing the distance between US probe and needle will allow determination of the maximum distance away from the needle at which tissue movement can be detected. Answering this question also may shed some light on the poorly understood concept of "acupuncture meridians," which are lines along the body "connecting" acupuncture points. Although comparing acupuncture and nonacupuncture points was not the focus of this study, we recently showed a correspondence between acupuncture meridians and intermuscular or intramuscular (IM) connective tissue planes (Langevin et al. 2002b) and proposed that propagation of mechanical

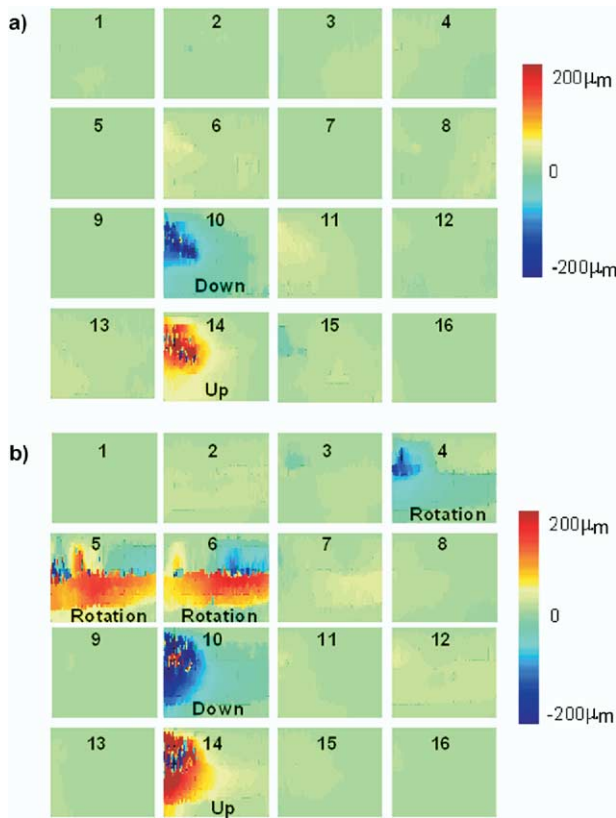


Fig. 5. Sequential displacement images of needle motion 2 with (a) no rotation and (b) rotation (16 revolutions). Every 4th frame is represented (or approximately every 0.3 s). The effect of rotation is apparent in (b) 4 to 6. The effect of downward needle motion is seen in frames (a)10 and (b)10, and that of upward needle motion in frames (a)14 and (b)14. Scale bar indicates tissue displacement in μm .

signals through connective tissue may be an important component of acupuncture’s therapeutic mechanism. It is, therefore, plausible that the maximum distance at which tissue mechanical stimulation occurs during needling may be greater along meridians and that this difference may underlie some of the rationale for the traditional practice of needling acupuncture points.

Our results also suggest that leaving the needle in the tissue for 5 min has the effect of loosening the needle/tissue mechanical bond. When the number of needle revolutions was set at zero, the only difference between needle motion 1 and needle motion 2 was the amount of time that the needle spent in the tissue, yet we observed a significant difference in tissue response between these identical successive longitudinal needle motions (Figs. 9 and 11 for zero rotation). The presence of the needle in the tissue (in effect creating a small wound) for this amount of time may cause some fluid exudation that may affect the biomechanical behavior of the tissue. Indeed, after 5 min, eight needle revolutions appeared necessary to reduce slippage to pre-

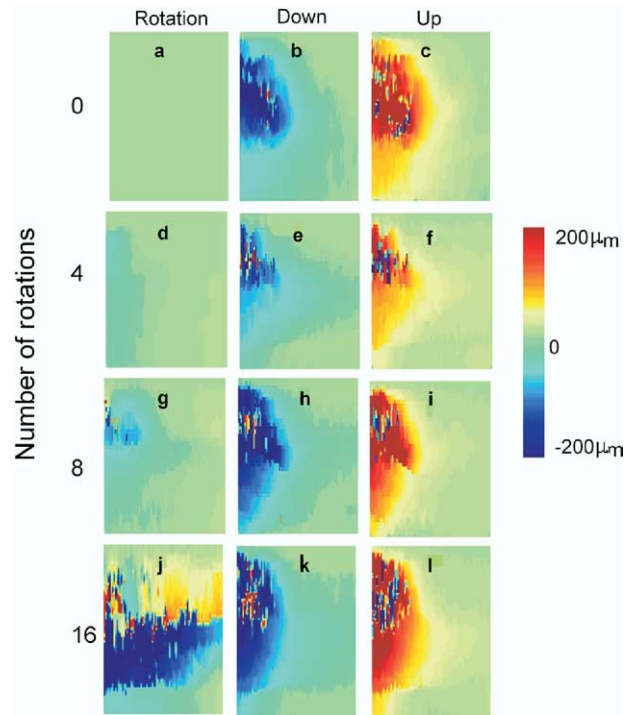


Fig. 6. Peak displacement images of needle motion 2 with (a)–(c) 0, (d)–(f) 4, (g)–(i) 8, and (j)–(l) 16 needle revolutions. Images represent peak tissue displacement during rotation (or lack thereof) (left column), downward (middle column) and upward (right column) needle motion. Scale bar indicates tissue displacement in μm .

rotation levels (Fig. 9). This suggests that rotation would have induced even more extensive tissue displacement, had the needle been rotated immediately after insertion.

An immediate clinical implication of this study is the demonstration that US elastography can objectively document tissue responses during acupuncture treatments. A key component of an acupuncturist’s skill is the ability to feel for what is happening in the tissue during needling. The acupuncturist traditionally relies on tactile sensations as he/she holds onto the needle handle and manipulates the needle in the tissue. The most basic of these sensations is that of tightening or grasping of the needle by the tissue (needle grasp). Other more subtle sensations are, for example, that of “emptiness” or “fullness” in the tissue when the needle is inserted. Based on these initial sensations, the acupuncturist uses different needling techniques (such as “tonifying” or “reducing”) and feels for a change in the tissue as a result of manipulation (for example, a sensation of emptiness may subside after a tonifying technique is applied). These needling techniques have been described in ancient Chinese texts for centuries but, until now, the effect of these techniques could not be objectively documented. To be able to see, record and analyze tissue changes during

Table 2. Needle torque, needle force and tissue displacement during needle motion 2 (during and after rotation) across points randomized to the four rotation conditions

		Randomized rotation conditions				Mean*	p value [†]	
		0	4	8	16			
Rotation	Torque (mNm)	0.004 ± 0.00	0.22 ± 0.02	0.34 ± 0.06	0.69 ± 0.02	0.31 ± 0.02	< 0.001	
	Disp (μm)	UL	-6.8 ± 2.2	-27.3 ± 4.9	-32.1 ± 4.4	-36.2 ± 5.6	-25.6 ± 2.1	< 0.001
		LL	-15.0 ± 4.5	-31.0 ± 4.1	-40.8 ± 4.8	-78.6 ± 18.6	-41.4 ± 5.3	< 0.001
		UR	-6.5 ± 2.1	-8.7 ± 1.79	-16.1 ± 5.4	-27.9 ± 9.9	-14.8 ± 2.9	0.008
		LR	-21.1 ± 4.1	-25.0 ± 3.2	-34.2 ± 7.8	-45.0 ± 7.3	-31.3 ± 3.1	0.006
Overall	-12.3 ± 3.1	-23.0 ± 2.5	-30.8 ± 5.0	-47.0 ± 9.5	-28.3 ± 2.9	< 0.001		
Downward needle motion	Force (N)	-0.27 ± 0.03	-0.43 ± 0.04	-0.47 ± 0.05	-0.57 ± 0.05	-0.43 ± 0.02	< 0.001	
	Disp (μm)	UL	-70.0 ± 7.5	-84.5 ± 9.1	-94.8 ± 9.6	-98.5 ± 10.9	-87.0 ± 4.1	0.020
		LL	-76.0 ± 10.6	-91.6 ± 8.4	-90.7 ± 10.1	-116.7 ± 12.1	-93.8 ± 5.1	0.010
		UR	-14.0 ± 2.2	-18.6 ± 3.1	-22.6 ± 4.2	-26.7 ± 3.8	-20.5 ± 1.2	< 0.001
		LR	-32.2 ± 4.8	-38.3 ± 4.4	-41.2 ± 3.6	-46.5 ± 7.0	-39.5 ± 2.5	0.057
Overall	-48.0 ± 5.2	-58.2 ± 5.6	-62.3 ± 6.0	-72.1 ± 6.7	-60.2 ± 2.8	0.005		
Rebound	Disp (μm)	UL	12.4 ± 2.5	6.7 ± 1.7	7.7 ± 1.6	1.7 ± 0.6	7.1 ± 0.9	< 0.001
		LL	15.4 ± 2.6	12.9 ± 2.7	9.0 ± 2.0	8.3 ± 2.2	11.4 ± 1.2	0.040
		UR	2.8 ± 0.9	1.1 ± 0.8	1.4 ± 1.0	2.1 ± 1.1	1.8 ± 0.4	0.801
		LR	9.3 ± 2.4	6.6 ± 2.4	6.2 ± 2.7	7.4 ± 2.9	7.4 ± 1.2	0.646
		Overall	10.0 ± 1.7	6.4 ± 1.7	6.1 ± 1.6	4.9 ± 1.6	6.7 ± 0.8	0.048
Upward needle motion	Force (N)	0.25 ± 0.03	0.37 ± 0.04	0.41 ± 0.06	0.65 ± 0.09	0.41 ± 0.02	< 0.001	
	Disp (μm)	UL	49.1 ± 7.2	58.8 ± 8.1	74.2 ± 8.4	76.5 ± 10.0	64.7 ± 3.5	0.006
		LL	53.4 ± 12.1	63.5 ± 9.9	67.7 ± 10.2	101.3 ± 13.8	71.5 ± 5.8	0.005
		UR	6.1 ± 1.4	10.5 ± 2.3	12.2 ± 3.0	17.3 ± 3.1	11.5 ± 1.0	< 0.001
		LR	17.9 ± 3.9	16.5 ± 3.1	19.4 ± 3.7	34.8 ± 6.8	22.1 ± 2.2	0.005
Overall	31.6 ± 5.0	37.3 ± 5.3	43.4 ± 5.1	57.5 ± 6.7	42.4 ± 2.6	0.001		

Values represent mean ± SE for $n = 12$ subjects.

Tissue displacement (Disp) measurements are shown for upper left (UL), lower left (LL), upper right (UR) and lower right (LR) ultrasound image quadrants, and for the four quadrants combined (overall); units of measurement are N (force), mNm (torque) and μ (disp).

* All means are significantly different from zero ($p < 0.001$).

† Significance associated with increasing or decreasing trend as a function of rotation.

needling, therefore, has the potential to open a new window onto the understanding of acupuncture and may improve future training of acupuncturists by providing

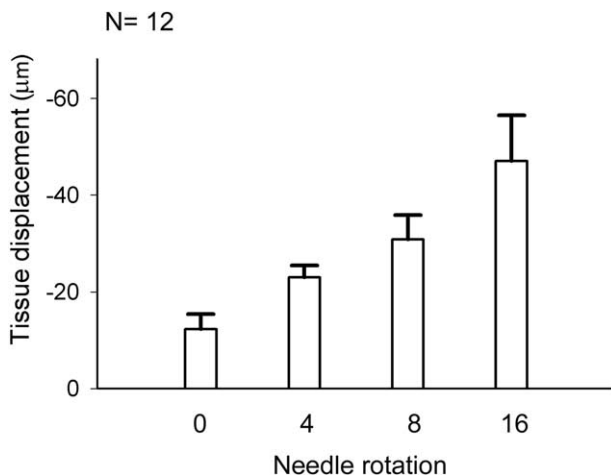


Fig. 7. Mean tissue displacement (averaged over the whole US image) during needle rotation. There was a significant ($p < 0.001$) linear increase in tissue displacement as a function of rotation. Results are shown as mean ± SE.

objective feedback that can be correlated with tactile sensations.

This study also constitutes an important first step into the ultrasonic investigation of tissue responses using a needle as a mechanical stimulus. Connective tissue is unique in that it forms a continuous network both around and within other tissues and may play an important role in the propagation of mechanical forces through the body away from the application point. This may have important applications in the display of tissue biomechanical properties, in particular, those related to connectivity between individual tissue components, the disruption of which may highlight disease. For example, the method described here can be used to compare the effect of the same needling stimulus in normal vs. pathologic tissue (such as inflammation, fibrosis or neoplasia). Another potential future application of this technique may be that of guiding needle biopsies. Real-time elasticity imaging is a promising new area of technological development. Biopsies performed under real-time elasticity imaging could use the tissue response to needling as a guide during needle advancement into the tissue (with or

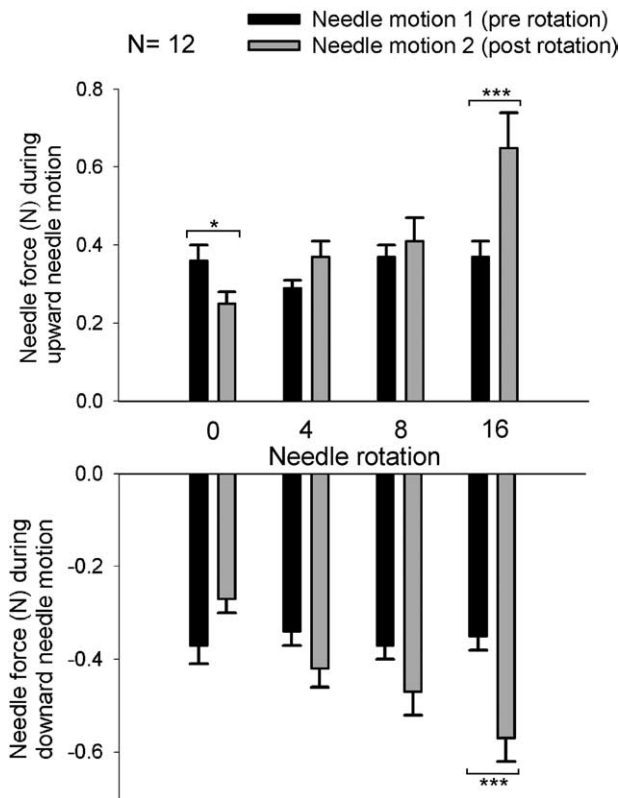


Fig. 8. Needle force measurements post needle rotation during needle motions 1 and 2. There was a significant ($p < 0.001$) linear increase in axial force as a function of rotation for both upward and downward needle motion for needle motion 2, but no significant linear increase for needle motion 1. Significance of difference between motions 1 and 2 is also shown: * $p < 0.05$; *** $p < 0.001$. Results are shown as mean \pm SE.

without additional needle rotation or up-and-down oscillation). A change in tissue displacement in response to needle motion may accompany insertion into the pathologic area (e.g., inflammation, neoplasia) and assist precise location of the biopsy sample.

We used elastographic techniques to estimate tissue displacement between successively acquired US frames. Due to the highly localized stimulus of the needle, tissue displacement was sufficient to depict the effect of the different types of needle manipulation at different distances from the needle. Future investigations will also include 2-D displacement (Konofagou and Ophir 1998) and strain estimation to determine the advantages of using multidimensional motion and deformation parameters and if image contrast increases as a result of strain mapping.

Cumulative displacement calculation confirmed that the magnitude of total vertical tissue displacement approached that of total vertical movement of the needle (Fig. 12). Incremental displacements were appropriate for our statistical analyses because our sig-

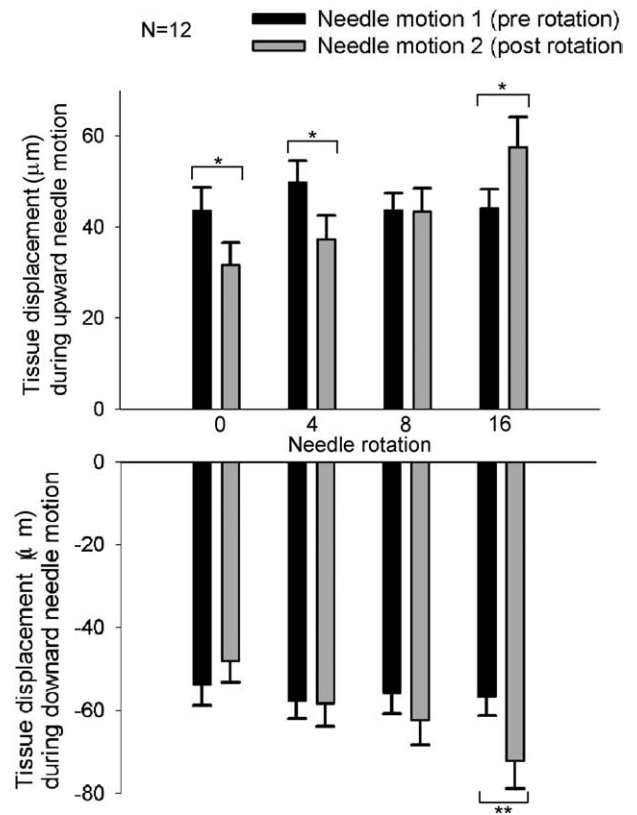


Fig. 9. Mean tissue displacement (averaged over the whole US image) during needle motions 1 and 2. There was a significant ($p < 0.001$) linear increase in tissue displacement as a function of needle rotation for both upward and downward needle motion for needle motion 2, but no significant linear decrease for needle motion 1. Significance of difference between motions 1 and 2 is also shown: * $p < 0.05$; ** $p < 0.01$. Results are shown as mean \pm SE.

nal-to-noise ratio (SNR) was high enough to test our hypothesis. Cumulative displacement images would be helpful, however, to perform precise spatial mapping of tissue motion during needling. Our previous studies in animals have shown that the amount of subcutaneous connective tissue winding around the needle during rotation correlated with the force necessary to pull the needle out of the skin (Langevin *et al.* 2002). Whether or not subcutaneous tissue also is primarily involved in humans (as opposed to perimuscular fascia or IM connective tissue) remains unknown. In this study, needle insertion depth was maintained constant at 28 mm. This resulted in varying degrees of needle muscle penetration across subjects, with some subjects having no muscle penetration at all. Further studies of needling using cumulative tissue displacement mapping and varying needle depths would be useful to determine precisely which type(s) of connective tissue is/are involved during needle rotation.

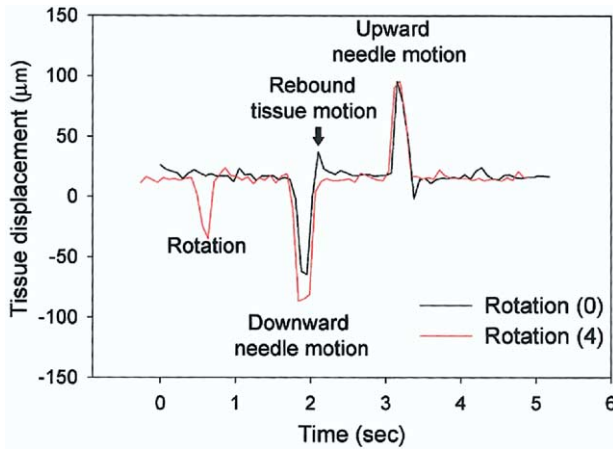


Fig. 10. Time plots of tissue displacement (averaged over the left upper quadrant of the US image) showing typical tissue behavior with needle rotation (4 revolutions) compared with no rotation. Negative tissue displacement is clearly seen during rotation. Tissue rebound after downward needle motion is apparent with no rotation, but not with rotation.

Although the acupuncture needle itself was not visible on the US B-scans, we did observe a nonuniform “imprint” of lower displacement (at a 45° angle in the upper left quadrant of the image) during needle motion, thus creating a “signature” image for the location of the needle (Fig. 6i, j). An imprint of greater displacement in the same location could also be seen in cine-loops when the needle was stationary. Possible causes for this tissue displacement, de-

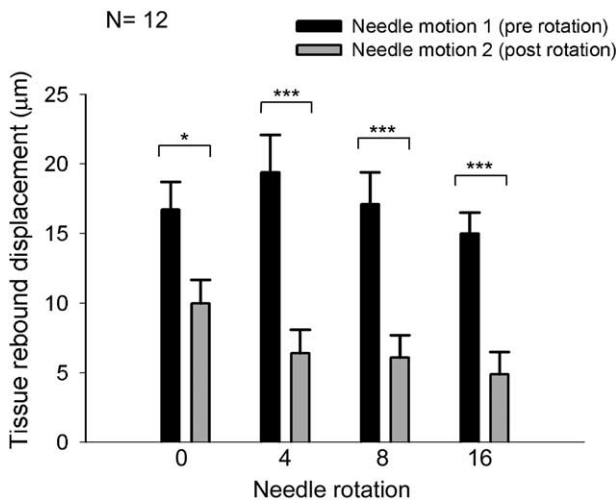


Fig. 11. Mean rebound tissue displacement (averaged over the entire US image) after downward needle motions 1 and 2. There was a significant ($p < 0.05$) linear decrease in tissue rebound as a function of needle rotation for needle motion 2, but no significant linear decrease for needle motion 1. Significance of difference between motions 1 and 2 is also shown: * $p < 0.05$; *** $p < 0.001$. Results are shown as mean \pm SE.

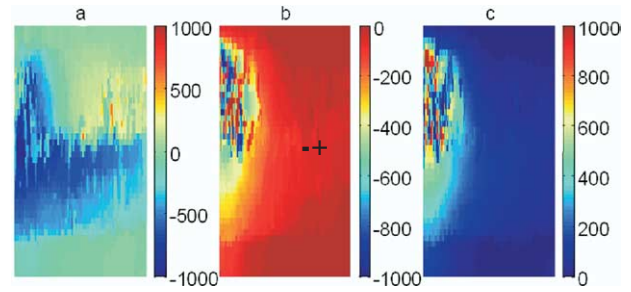


Fig. 12. Cumulative tissue displacement during (a) needle rotation (16 revolutions), (b) downward and (c) upward needle movement. In this case, for downward and upward needle movements, cumulative displacement amplitude averaged over a 1 mm \times 1 mm area near the needle was -1.32 mm and 1.46 mm, respectively. Cumulative tissue movement amplitude, therefore, approached the magnitude of the axial component of the needle movement vector (1.41 mm) (see Fig. 3b). Scale bar indicates tissue displacement in μm .

spite the assumed immobility of the needle, may be slight jittering of the needle when needle motion is at zero, or tissue movement near the needle due to tissue responses to needling. The latter may be related to the observation that the duration of the presence of the needle inside the tissue affects the amount of tissue displacement during needle motion.

In conclusion, we have shown that acupuncture needle rotation modifies the biomechanical behavior of soft tissue during subsequent upward and downward needle motion. Mechanical stimulation of tissue during “lifting and thrusting” of the needle and potentiation of this stimulation by needle rotation are important components of acupuncture therapy. The above-described imaging technique may prove to be key to monitoring these effects and open up a new way to explore the physiological phenomena associated with acupuncture. In addition, our study’s broader potential implications stem from the demonstration that tissue needling creates characteristic movement patterns that can be recorded and analyzed. Disruption of these patterns may occur in pathologic conditions. Thus, the technique presented in this paper may become an important tool to investigate and eventually to diagnose specific types of tissue pathology and may be useful during other types of needling, including biopsies.

Uncited references

NIH (National Institutes of Health). Acupuncture: NIH consensus statement. Vol. 15. Bethesda, MD: NIH, 1997:1–34.
 BMA (British Medical Association Board of Science and Education). Acupuncture: efficacy, safety and practice. London: Harwood Academic Publishers, 2000.

Cheng X. Chinese acupuncture and moxibustion. Beijing: Foreign Language Press, 1987.

Ernst E. Clinical effectiveness of acupuncture: An overview of systematic reviews. In: Ernst E, White A, eds. Acupuncture: A scientific appraisal. Oxford: Butterworth-Heinemann, 1999.

Helms JM. Acupuncture energetics—A clinical approach for physicians. Berkeley: Medical Acupuncture Publishers, 1995.

Tait PL, Brooks L, Harstall C. Acupuncture: Evidence from systematic reviews and meta-analyses. Alberta, ONT, Canada: Alberta Heritage Foundation for Medical Research, 2002.

Vickers A. Acupuncture: Effective health care. NHS Centre Rev Dissem 2001;7:1–12.

Yang J. The golden needle and other odes of traditional acupuncture, 1601 Translated by Bertschinger R. Edinburgh: Churchill Livingstone, 1991.

Acknowledgements—We thank Jason A. Yandow and Nicole A. Bouffard for technical assistance and Debbie Stevens-Tuttle for assistance with subject recruitment. We also thank GE Medical Systems for use of the System FiVe Ultrasound scanner. This study was funded by the National Center for Complementary and Alternative Medicine (NCCAM) (Grants R21-AT00300 and RO1-AT01121), and conducted at the University of Vermont General Clinical Research Center at Fletcher Allen Health Care supported by the NIH Grant M01RR00109. Its contents are solely the responsibility of the authors and do not necessarily represent the official views of NCCAM, or the National Institutes of Health.

REFERENCES

Barannik EA, Girnyk A, Tovstiak V, et al. Doppler ultrasound detection of shear waves remotely induced in tissue phantoms and tissue *in vitro*. Ultrasonics 2002;40:849–852.

Hein IA, O'Brien Jr WD. Current time-domain methods for assessing tissue motion by analysis from reflected ultrasound echoes—A Review. IEEE

Konofagou EE, Hynynen K. Localized harmonic motion imaging: Theory, simulations and experiments. Ultrasound Med Biol 2003; 29(10):1405–1413.

Konofagou EE, Ophir J. A new method for estimation and imaging of lateral strains, corrected axial strains and Poisson's ratios in tissues. Ultrasound Med Biol 1998;24:1183–1199.

Krouskop TA, Wheeler TM, Kallel F, Garra BS, Hall T. Elastic moduli of breast and prostate tissues under compression. Ultrasonic Imaging 1998;20(4):260–274.

Langevin HM, Yandow JA. Relationship of acupuncture points and meridians to connective tissue planes. Anat Rec (New Anat) 2002; 269:257–265.

Langevin HM, Churchill DL, Cipolla MJ. Mechanical signaling through connective tissue: A mechanism for the therapeutic effect of acupuncture. FASEB J 2001a;15:2275–2282.

Langevin HM, Churchill DL, Fox JR, et al. Biomechanical response to acupuncture needling in humans. J Appl Physiol 2001b;91:2471–2478.

Langevin HM, Churchill DL, Wu J, et al. Evidence of connective tissue involvement in acupuncture. FASEB J 2002;16:872–874.

Levinson SF, Shinagawa M, Sato T. Sonoelastic determination of human skeletal muscle elasticity. J Biomech 1995;28(10):1145–1154.

Montgomery DC. Design and analysis of experiments. 3rd ed. New York: John Wiley, 1991:649.

Nightingale KR, Palmeri ML, Nightingale RW, Trahey GE. On the feasibility of remote palpation using acoustic radiation force. J Acoust Soc Am 2001;110(1):625–34.

O'Connor J, Bensky D. Acupuncture, a comprehensive text (Shanghai College of Traditional Medicine). Seattle: Eastland Press, 1981.

Ophir J, Alam SK, Garra BS, et al. Elastography: Ultrasonic estimation and imaging of the elastic properties of tissues. Proc Inst Mech Eng Part H 1999;213:203–233.

Ophir J, Cespedes I, Ponnekanti H, Yazdi Y, Li X. Elastography: A quantitative method for imaging the elasticity of biological tissues. Ultrason Imaging 1991;13:111–134.

Walker WF, Fernandez FJ, Negron LA. A method of imaging viscoelastic parameters with acoustic radiation force. Phys Med Biol 2000;45(6):1437–1447.